JMEPEG (2009) 18:664–671
DOI: 10.1007/s11665-009-9384-z

1059-9495/$19.00

Carbon Fiber Reinforced Smart Laminates with Embedded SMA Actuators—Part I: Embedding Techniques and Interface Analysis

P. Bettini, M. Riva, G. Sala, L. Di Landro, A. Airoldi, and J. Cucco

(Submitted October 21, 2008; in revised form December 19, 2008)

Up to now one of the main limits for a large use of shape memory alloys (SMA)-based smart composite structures in the aerospace industry is the lack of useful numerical tools for design. Moreover, technological aspects still need a more detailed investigation. This paper shows how to overcome issues regarding embedding of NiTiNOL wires in carbon fibre/epoxy laminates. A crucial aspect of those structures is related to the load transfer capabilities between the SMA actuators and the host material during their activation. Embedding techniques developed for taking into account problems like thermal and electrical compatibility between actuators and host material and passive/active invasivity are reported in this paper. Simple smart laminates with several actuators were manufactured, tested, and deeply analyzed. In order to characterize the interface in the real operative conditions, pull-out tests were conducted on NiTiNOL wires embedded in composite fiber laminates. The results were compared to standard experiments on wires embedded in pure epoxy resin blocks.

Keywords embedding technologies, interface analysis, NiTiNOL, pull-out, smart composites structures

1. Introduction

Materials for primary structures in aerospace applications must have high mechanical properties, lightness, and durability. It is important for these structures to exhibit good behavior in terms of impact resistance, environmental endurance, fire and corrosion resistance. Composite materials meet well such requirements and nowadays are widely used in many engineering fields.

On the other hand, a large number of new materials and technologies (i.e. micro-electronic devices, shape memory alloys (SMA)-based micro-actuators, piezo-ceramics (PZT), electro-active polymers, optical fibers (OF), etc.) allow to imagine extensive diffusion of smart materials in many aerospace and ground applications. Their capabilities in terms of shape and vibration control of large space structures, acoustic control for noise reduction in civil aircraft, health monitoring and in-site structure identification are well assessed and promising results are also obtained in many other applications.

In the last years, several research activities in the manufacturing processes field have been devoted to develop smart structures that could combine high mechanical efficiency, due to composite host materials, with good functional properties of the embedded sensors and actuators (Ref 1-3).

The embedding of these smart devices into the structures could give some advantages compared to their bonding onto the outer skin. For example, they allow the actuation in locations hardly accessible from outside because of shape constraints; the protection of the actuation system inside host structure from all environmental effects, which may reduce its performance, can be also achieved. In addition, active structures could be applied even in those cases where a clean and smooth surface is required (i.e. aerodynamic surfaces) (Ref 4).

Abbreviations	
A_s, A_f	austenite start and finish temperature
CFRP	carbon fiber reinforced plastic
CFRSL	carbon fiber reinforced smart laminates
CTE	coefficient of thermal expansion
DOF	degree of freedom
FE	finite element
GFRP	glass fiber reinforced plastic
HF	hydrofluoric acid
M_s, M_f	martensite start and finish temperature
OWSME	one way shape memory effect
OF	optical fiber
PZT	piezo-ceramic
QP	quick-pack
SMA	shape memory alloys
TWSME	two way shape memory effect
T_g	glass transition temperature
UD	uni-directional laminate

This article is an invited paper selected from presentations at Shape Memory and Superelastic Technologies 2008, held September 21-25, 2008, in Stresa, Italy, and has been expanded from the original presentation.

P. Bettini, M. Riva, G. Sala, L. Di Landro, A. Airoldi, and **J. Cucco**, Department of Politecnico di Milano, Aerospace Engineering, Milan, Italy. Contact e-mail: riva@aero.polimi.it.

The embedding technique of these components within the load-carrying structure is still a leading edge issue. Research activities oriented both to the development of manufacturing techniques, to the characterization of embedded sensors and to the estimation of actuators invasivity (active and passive) on the smart structure performance are of valuable importance.

Moreover, most of the applications are strongly dependent on the availability of useful numerical tools. In fact, all the design activities regarding structures are nowadays related to the adoption of numerical models able to predict the efficiency and performance of the systems (Ref 5). The peculiarity of the smart composite structures underlines this problem due to the joined complexity of the active materials behavior (non-linearity) with the composite material modelling (anisotropy, damage mechanisms).

The activity of the Smart Composite Laboratory at Politecnico di Milano is dedicated to the development of both technological processes and numerical tools for Smart Carbon Laminates with embedded sensors and actuators. Some of the results are presented in this paper. In a further paper, modelling and numerical analysis of embedded SMA will be presented. This activity is focused on the embedding of Shape Memory wires, selected taking advantage of their functional properties in terms of low activation speed combined with high loading capability. In fact, these characteristics are useful for most of the aerospace applications (airfoil morphing, shape control, etc.). Shape Memory effect of these actuators can be exploited in two different ways. In the first one, wires are embedded in a detwinned martensite phase and the activation of the structure is obtained using the one way shape memory effect (OWSME) due to the reverse transition induced by heating (from detwinned martensite to the austenite phase); then the structure (and the embedded wires too) come back to the initial form through its stiffness (host material remain in the elastic range) when the wires are cooled and the forward transition is induced. In the second one, wires can be embedded both in austenite or in detwinned martensite phase considering two way shape memory effect (TWSME). A structure can change its form by heating or cooling so that reverse or forward transition, respectively, occurs (Ref 6, 7).

In any case, the coupling between SMA and host material poses a number of critical aspects which have to be taken into account during the embedding process. This paper presents the development of technological process and the investigation of the interface between active SMA and host materials in case of carbon fiber reinforced plastic (CFRP) laminates. A first aspect is related to the curing temperatures of the thermoset epoxy matrices used in aeronautical composites; often these are higher than the transition temperatures of standard achievable actuators so that both reverse and forward transition occur during the curing process. A second aspect is related to the activation of the wires. Joule heating requires electrical insulation between wires and CFRP host material. Finally, a good adhesion of the resin around the actuators has to be obtained to guarantee high levels of load transfer capability.

The objective of this work, together with what will be presented in a further paper oriented to the development of useful numerical tools for SMA-based micro-actuators, is the definition of a design strategy that takes into account the computational costs and the level of accuracy required by a smart structure for a preliminary prediction of the overall performance of the system.

2. Technological Aspects

2.1 Materials Choice

Ideal smart structures should exhibit high mechanical performance and good functional properties keeping at the same time very low invasivity of the embedded actuators. If such a design concept is considered, a trade-off between actuators dimensions and the host material stiffness is always required. For instance, in case of uni-directional laminates, wires SMA actuators with diameter comparable to the single ply thickness (125 μm) should be embedded with the same orientation as reinforcing fibers to minimize their invasivity. On the other hand, this configuration usually leads to a restrained activating power considering the high stiffness of this host material (due to very high content of fibers). To improve the activation efficiency while keeping a low invasivity, new technologies are being developed oriented toward the increasing of the volume fraction of SMAs in the laminate by substituting part of the reinforcing fibers with thin NiTiNOL wires at a single ply level.

The material choice is also dependent on the thermo-mechanical compatibility between the actuators and standard epoxy resin used for CFRP in aeronautical field. In particular, SMAs with A_f lower than the resin T_g have to be used to avoid a reduction of the stiffness of resin and interface; at the same time, A_s must be higher than normal operating condition temperatures of the smart structure in order to avoid undesirable activations. In addition, it is useful to have M_f greater than room temperature to avoid the use of a cooling system (i.e. Peltier) for the complete forward transition (Ref 8).

In order to maximize the activation effects, a host material with limited stiffness and actuators with relatively high diameters were thus chosen for this work. A previous research on embedded OF showed that their passive invasivity over the host material mechanical properties was negligible in static conditions (Ref 9). Considering the similarity between OF and SMA wires in terms of dimensional and morphological characteristics, the invasivity of thin NiTiNOL wires was assumed negligible. As a consequence, attention has to be paid only to the thermal loads during the activation that must keep safe the resin around wires. NiTiNOL wires with 381 μm diameter (Dynalloy) and fabric prepreg of 120 μm of thickness (Seal) were then selected. Their properties are summarized in Table 1 and 2, respectively.

2.1.1 Characterization of the Materials. A preliminary thermo-mechanical characterization of the SMA actuators was done to determine the mechanical properties, the transition temperatures and their stress dependency (Ref 10, 11). Results showed a multistep forward transition due to the presence of the

Table 1 Characteristics of SMA actuators as-received (transitions evaluated by DSC)

Material type	NiTiNOL $Ni_{52}Ti_{48}$
Shape	Wire
Dimensions	0.3181 mm
A_s-A_f	41.23-69.60 °C
M_s-M_f	19.67-3.91 °C
R_s-R_f	72.95-39.98 °C
E^A	68 GPa
E^M	21 GPa
E^R	14 GPa

Table 2 Characteristics of the host material

Material type	Carbon fabric prepreg SEAL CC90 ET443
Cured thickness ply	0.12 mm
Curing temperature	125 °C
T_g	127 °C
$E_{xx} = E_{yy}$	56.55 GPa
ν_{yx}	0.0514
G_{xy}	4.043 GPa

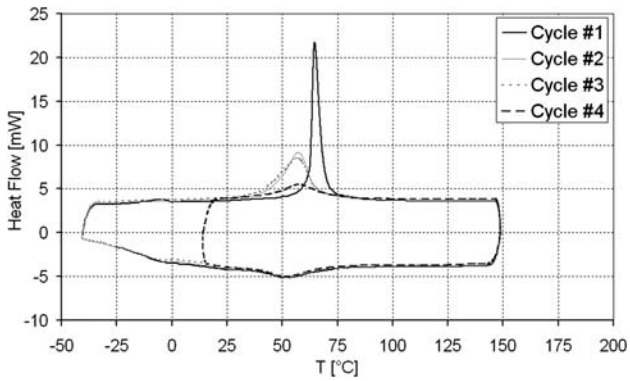

Fig. 1 DSC analysis of the Dynalloy SMA actuators: determination of transition temperatures without stress applied by using heat flow curves (Exo Up)

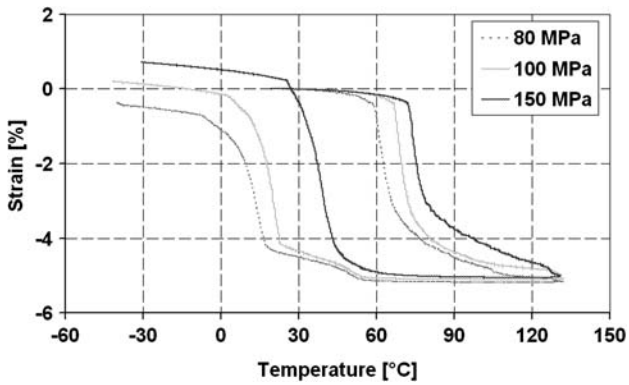

Fig. 2 Strain vs. temperature curves of SMA trained wire detwinned at 4% at different loading levels

R-phase that can be removed by an annealing treatment (Ref 12). DSC analyses were performed and the transition temperatures were evaluated from the curves adopting the method suggested by ASTM standard (Table 1) (Ref 13). Figure 1 shows the results obtained with the SMA wire as-received. The superposition of all the scanning cycles (after the first one) confirms the good quality of the analyses. The scanning n°4 (dashed line) underlines that A_s and A_f do not change even if the reverse transition start in the R-phase condition.

Typical strain versus temperature curves with different applied stress obtained by using a Dynamic Mechanical Analyzer are reported in Fig. 2. It can be observed that R-phase disappears when high stresses are imposed. Stress dependence of the Dynalloy SMA transition temperatures experimentally obtained is summarized in Fig. 3. Young

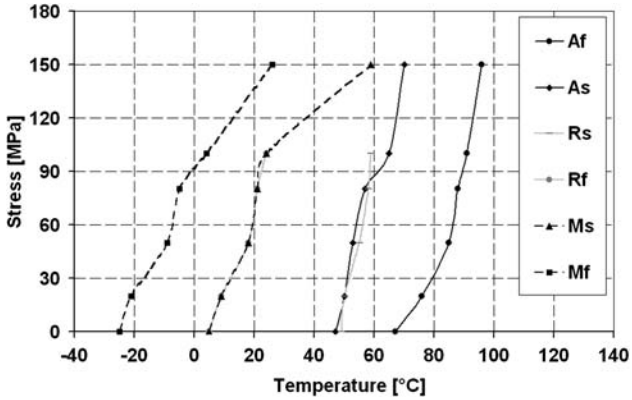

Fig. 3 Stress dependence of the Dynalloy SMA transition temperatures obtained using a Dynamo Mechanical Analyzer

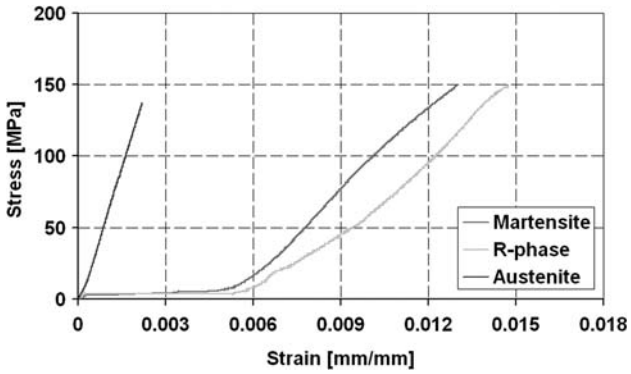

Fig. 4 Stress vs. strain curves of the SMA wires obtained in the three different phases with a Dynamo Mechanical analyzer

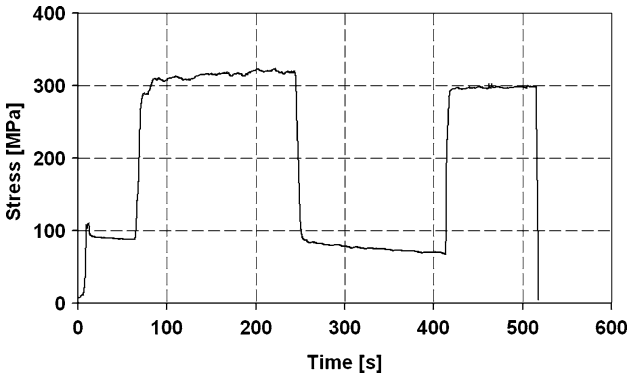

Fig. 5 Iso-length test on wire detwinned at 4%: SMA exhibits about 300 MPa of recovery stress

moduli in the three different phases were evaluated through tensile tests (Table 1). The obtained stress-strain curves (Fig. 4) are limited to 150 MPa corresponding to the load cell limit of the loading device (18 N). To evaluate SMAs recovery stress, iso-length tests were also performed on 4% pre-strained wires by using an electromechanical dynamometer machine (INSTRON). The test implies two cycles of turning on and switching off the power supply for Joule activation to verify the repeatability of the performance. Results are shown in Fig. 5.

Finally, tensile specimens according ASTM D3039 were manufactured and tested in order to obtain the mechanical characteristics of the host material (Table 2). A DSC analysis was also performed to evaluate the cured resin glass transition temperature (Ref 14).

2.2 Embedding Technique

In order to manufacture a smart panel based on OWSME using the chosen materials, SMA wires have to be embedded in their martensite detwinned phase. A direct free embedding in CFRP is not possible due to the transition induced by the resin curing cycle.

One of the first methods developed to overcome this limit consisted in using special sheaths where the wires could pass into after the resin curing stage; the wires were then externally connected to the panel to give them load transfer capabilities (Ref 2, 15). This solution presents more drawbacks than benefits: very high invasivity, presence of an external device for the wires-structure connection and consequent less compact laminate with lower aerodynamic capacities when used as aeronautical shell. The technique developed in this research consists in a direct embedding of SMA wires with constraints that prevent the shrinkage due to the reverse transition. Doing so, a transient stress is induced on the constrained wires when the reverse transition occurs during the heating step of the resin curing cycle. After the polymer crosslinking, this state-of-stress gets off when the SMA comes back in martensite phase during the final cooling step of the cycle. At the end, the adhesion between embedded wires and the host material matrix gives the mutual load transfer capability without using external devices. If such an embedding technique is applied, the actuators efficiency strongly depends on the quality of this bonding. For this reason, the interface analysis, which is a crucial task, is required.

At the end of the process the wires are exiting the final laminate. If the activation is given by thermal convection or radiation (using hot air flow or electrical resistances), the edges of the panel can be trimmed removing the resin squeeze-out and the wire ends. On the other hand, if Joule-effect activation is used, the wire tips must be connected to the power supply system thus limitating the possibility of profiling the laminate. A special mold with elastomeric dams was designed and manufactured so that good quality edges can be guaranteed. In addition, dedicated connectors have simplified the activation system allowing the wires to be cut.

Figure 6 shows some details of the described technique. They are related to the manufacturing of a smart panel embedding six SMA. The Joule-activation in itself also requires an electrical insulation to avoid shorts between the host material and the embedded wires. This problem was solved adopting a glass fiber reinforced plastic (GFRP) insulating sub-laminate (named Quick-Pack (QP)) originally developed to embed different sensors or actuators (Ref 4, 9).

2.3 Quick-Pack

Quick-Pack is a thin laminate made of two fabric plies of glass fibers and epoxy matrix originally developed to protect OF sensors and PZT actuators during their embedding in a host material. With this preliminary process the very fragile OF or PZT result easier to handle. The result is a powerful system ready to be embedded (Ref 4, 9).

A preliminary validation of this QP technique for SMA wires was performed by accuracy and efficiency tests. Fatigue

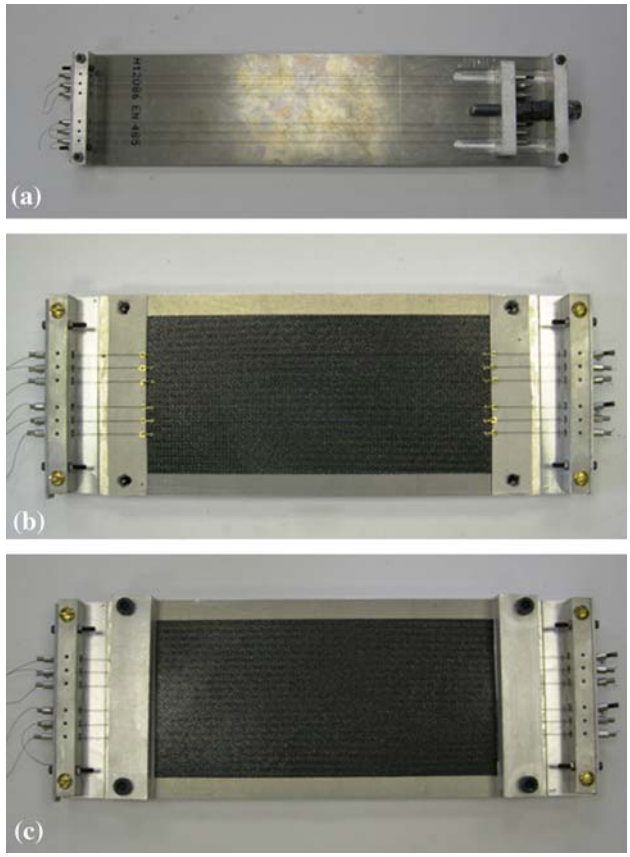

Fig. 6 Direct constraint embedding technique for SMA detwinned wires: pre-strain tool (a), constraining mechanism, crimp and elastomeric dams adopted during the lamination phase (b) and the whole system ready to be cured (c)

tests were included in a previous research activity on OFs (Ref 9). The porting of this technology for SMA actuators was done using NiTiNOL wires embedded in a 50 μm of thickness GFRP/epoxy fabric with 66% of resin content of the same type used in the CFRP host material. The choice of the QP prepreg was done in order to minimize its invasivity. On this basis very thin prepreg with high resin percentage were selected so that limited cross section dimension changes and improvement of the adhesion between wires and plies can be obtained.

After the manufacturing of the QP, its final embedding in the host material requires subsequent thermal processes; these do not degrade the polymer characteristics; since should be assumed as post-curing processes which should usually lead to improved stability and mechanical performance. On the other hand, different coefficient of thermal expansion (CTE) between GFRP and CFRP may induce residual stresses inside the laminate. Fatigue tests carried out in the previously mentioned work demonstrated that the presence of this new device does not create any significant degradation of the final structure (Ref 9).

The QP tips are a further critical issue because they must exit the CFRP panel to avoid shorts. For this reason, special elastomeric pads were used during the final curing to improve layers compaction.

The carbon fiber reinforced smart laminates (CFRSL) based on NiTiNOL micro-actuators obtained at the end of the whole process (Fig. 7) was used for experiments and numerical

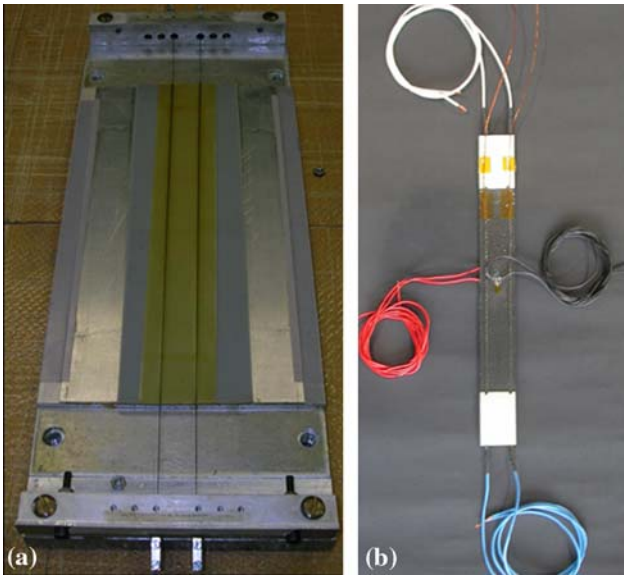

Fig. 7 Quick-Pack manufacturing phase (a) and final CFRSL specimen (b)

Table 3 Characteristics of manufactured CFRSL

Specimen ID	003
Dimensions	260 × 40 × 1.27 mm
Host material	Carbon fabric prepreg SEAL CC90 ET443
Cured thickness ply	0.12 mm
Lamination sequence	$[90°/(0°)_2/90/45°/-45°]_s$
Actuators material	Dynalloy wires of 0.381 mm diameters
Number of actuators	2

correlations that will be presented in a further paper. The main characteristics and dimensions of this panel are summarized in Table 3.

3. Interface Analysis

The efficiency of a smart structure is strongly dependent on the interface between the sensors/actuators and the host materials. Their adhesion is an essential requirement to ensure congruence and high load transfer capability. The same considerations have always driven the advance of composite materials and several methods have been developed to study the interface between reinforced fibers and matrix (like microtension, fragmentation, microcompression, pull-out tests) (Ref 16).

These methods can be independently used to evaluate the maximum interfacial shear stress (IFSS) that gives the interface failure and to understand its failure mechanisms. Pull-out test was selected for this work due to its simple set-up and specimens manufacturing phase (Ref 17).

Specimens are made up of small resin blocks with a single fiber embedded for a length (L) that must be less than a critical value (L_c); the critical length is defined as the embedded length that gives a pull-out force equal to the fiber failure one. In such a way debonding occurs instead of fiber failure (Fig. 8a). The average value of maximum shear stress (τ_{IFSS}) is obtained from

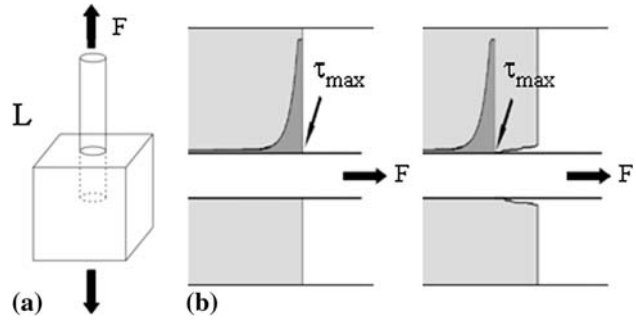

Fig. 8 Standard pull-out test to evaluate the IFSS between fiber and resin of the composite materials: specimen scheme (a) and failure mechanism (b)

the tests by using an equilibrium relationship based on a simplified stress distribution at the interface (Ref 17):

$$\tau_{IFSS} = \frac{F_{max}}{\pi \cdot d \cdot L}$$

where F_{max} is the maximum recorded force corresponding to the debonding and d is the fiber diameter.

Two observations can be done. First, this formula underestimates the stress levels since it considers a uniform state-of-shear-stress along the interface in the fiber direction. In fact, the failure propagation mechanism implies much different stress conditions as shown in Fig. 8(b). The fracture nucleates and propagates due to a peak of stress localized at the propagation front. Second, the friction forces between resin and fiber are neglected. Their evaluation could be done considering both friction coefficients and pressure at the interface due to technological cycles but they are very difficult to be obtained (Ref 18).

Pull-out tests on standard and non-standard specimens with SMA embedded wires are presented next. A hydrofluoric acid (HF) surface treatment was also performed on the embedded wires to evaluate the possible improvement of the adhesion between resin and wires.

In view of the fact that the presence of reinforcing fibers in the composite laminates as well as the high pressures applied during a typical prepreg curing cycles may strongly influence interface characteristics (Ref 19), a particular kind of non-standard specimens was also manufactured and tested in order to analyze the interface in the real operative conditions of the wires.

3.1 Standard Pull-Out Tests

3.1.1 Specimens Manufacturing and Tests Set-up. Specimens were made with an Araldite LY5052/Aradur 5052 epoxy resin. A curing cycle of 3 h at 100 °C was chosen in order to have the glass transition temperature (130 °C) higher than NiTiNOL A_f. All the wires were embedded in their austenite phase for a length of about 2÷3 mm. During the manufacturing phase a particular attention was used to eliminate voids in the resin and to avoid its rising up along the wires at the exit of the blocks. After a degassing process, the resin was poured in a special aluminum mold equipped with a drilled PTFE plate for the wires crossing. Moreover, the mold had a flexible wall to prevent possible residual stresses due to curing cycles (Fig. 9). At the end of curing all the specimens were cooled down to

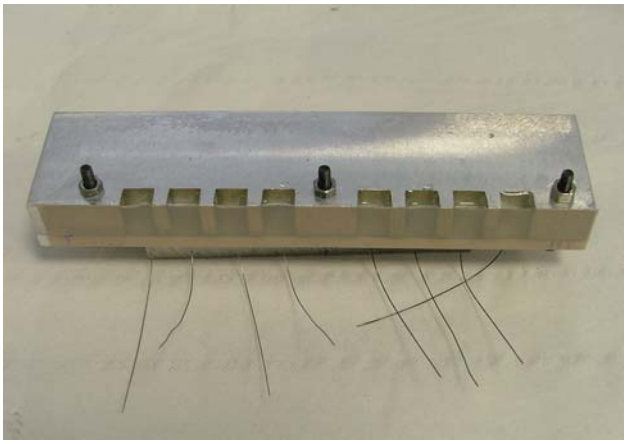

Fig. 9 Special mold for the pull-out specimens manufacturing

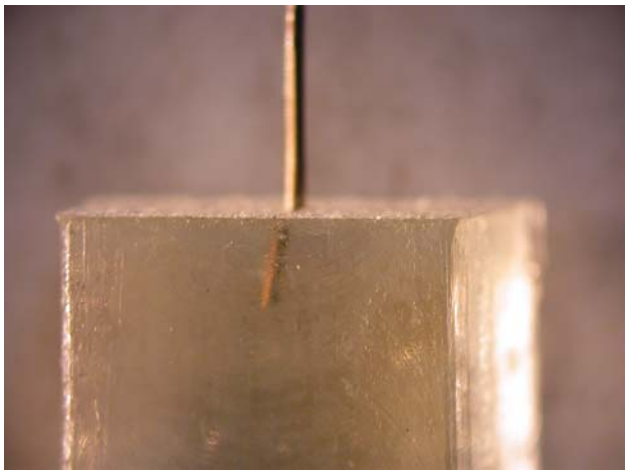

Fig. 10 Detailed view of a standard pull-out specimen showing the absence of resin rising

ensure martensite phase in the wires. A detailed view of a manufactured specimen shows the absence of the rise up (Fig. 10).

A specific testing equipment was also designed and manufactured to apply the restrained top loading method so that pre-load stresses on the resin blocks due to the test machine clamping can be avoided. The tools were made of CFRP plies covered by two GFRP plies that fulfill the electrical insulation (required in the Joule-activation of the wires adopted for non-standard specimens).

Two set of specimens were tested at low and high temperature to evaluate the IFSS in martensite and in austenite phase, respectively. All the tests were performed using a mono-axial electro-mechanical testing machine (INSTRON 4302) in displacement control mode with crosshead speed of 0.5 mm/min equipped with a 1 KN cell load and a thermal chamber (Fig. 11).

3.1.2 Results of Standard Pull-Out Tests. Results are summarized in Fig. 12 that reports the force versus displacement curves referred to all the different sets (martensite with and without HF surface treatment, austenite). All the pull-out tests led to complete debonding: the load rises until debonding and then a sudden drop occurs; afterward the effects of friction

Fig. 11 Pull-out equipment: the tensile tools are clamped and installed in the environmental chamber

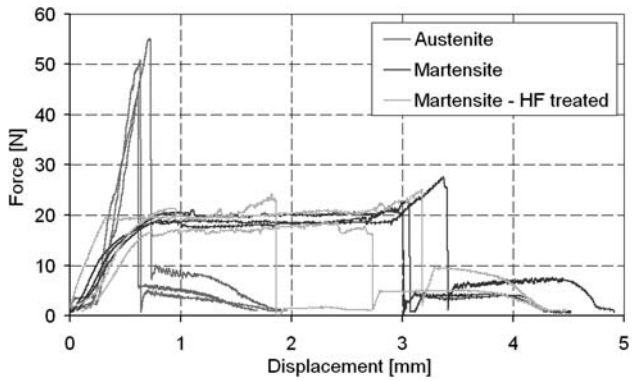

Fig. 12 Pull-out curves of standard specimens in all configurations (austenite, martensite and martensite—HF treated)

between wire and resin are evidenced by a slightly varying force. In the martensite test, the debonding occurs at higher loads than those leading to stress induced martensite (SIM) underlined by the presence of a plateau. The comparison between the curves referred to HF treated and not treated wires does not show appreciable differences.

On the other hand, in austenite tests, the debonding loads are higher than in martensite ones. This behavior could be related to the thermal mismatch between resin and metal which affects the mechanical constraint on the wires, or to a variation of wire roughness consequent to phase transformation.

Figure 13 shows IFSS obtained from all experimental tests and it underlines the SMA phase influence on the interface. Even if experimental data are limited for a reliable statistical analysis, the low standard deviation obtained permits to evaluate a meaningful average of IFSS reported in Table 4. It can be seen that austenite IFSS (20.05 MPa) is three times larger than the martensite one (7.59 MPa) while the interface is not significantly influenced by the HF treatment (6.67 MPa).

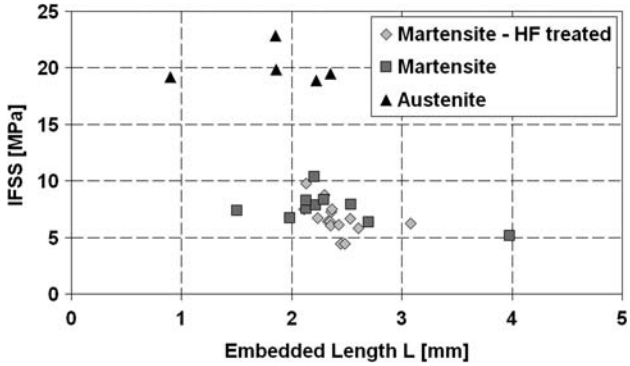

Fig. 13 IFSS obtained in the standard pull-out tests. Comparison between martensite, martensite with hydrofluoric acid surface treatment and austenite phases

Table 4 IFSS obtained from standard pull-out tests

Type of specimens	IFSS, MPa
Martensite—HF treated	
Number of data	15
Average IFSS	6.67
Standard deviation	1.35
Martensite	
Number of data	10
Average IFSS	7.59
Standard deviation	1.32
Austenite	
Number of data	15
Average IFSS	20.05
Standard deviation	1.43

3.2 Non-Standard Tests

3.2.1 Specimens Manufacturing and Tests Set-up. Non-standard pull-out tests were considered in order to evaluate the interface in operating conditions. To achieve this goal, a set of specimens made of a CFRP fabric laminate embedding a single martensite detwinned SMA wire deformed with 4% of strain was designed and manufactured using the technologies previously described in this paper (Fig. 14a). Finally special tabs were bonded at room temperature to ease clamping to the testing machine (Fig. 14b).

The specimens were manufactured in series of two by modifying the tools used for the curing of the smart laminates (Sect 2.2). As a consequence, a loss of repeatability in terms of geometrical and physical characteristics must be taken into account during the analysis of results.

Standard methods for the IFSS determination cannot be adopted in this configuration because of the wires exiting the specimens. Thus, estimation of interface quality can be based only on the overall pull-out force applied to extract the wires. As in previous standard tests, specimens were tested at low and high temperature adopting a thermal chamber (Fig. 14c). A different specimen series was tested by Joule-activation maintaining a fixed crosshead position in order to evaluate the wires loading capacity.

3.2.2 Results of Non-Standard Pull-Out Tests. Results of the tensile tests are reported in Fig. 15: again austenite interface results are stronger than martensite one. In this

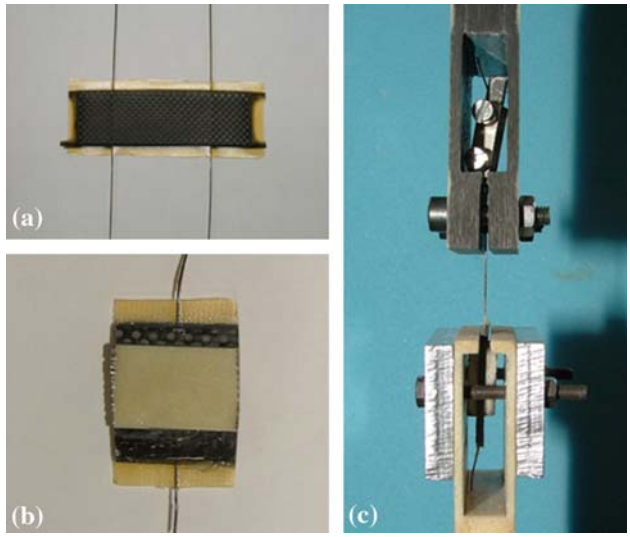

Fig. 14 Non-standard pull-out specimen manufacturing and test set up: specimen after the curing (a), after the gluing of tabs (b) and installed in the test facility (c)

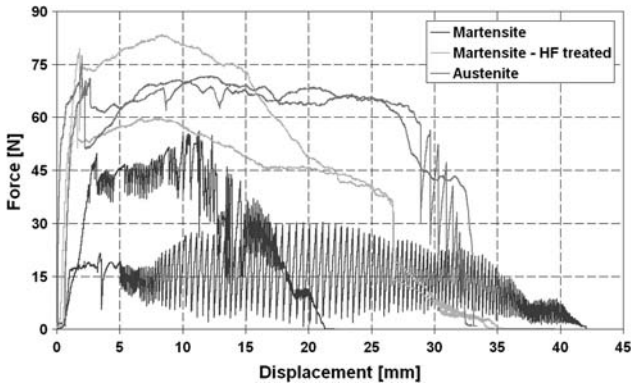

Fig. 15 Pull-out curves of non-standard specimens in all configurations (austenite, martensite and martensite—HF treated)

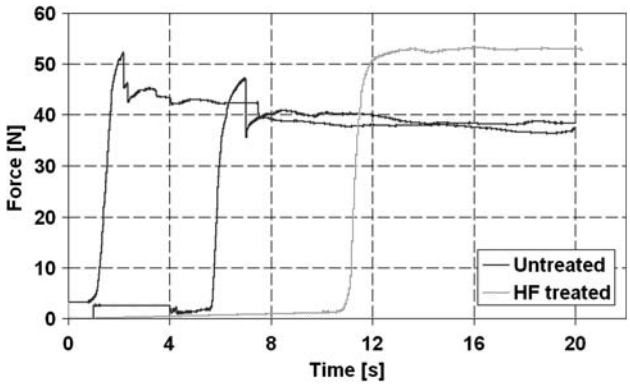

Fig. 16 Joule activation of non-standard specimen: untreated and HydroFluoric treated

situation, the HF treatment seems to effectively improve the bonding performance between actuator and host material. In fact, the martensite-HF treated curves are similar to the austenite ones both up to the debonding peak load and in the

following wire slipping out stage. The reason of this behavior could be due to a possible roughness variation or to higher wettability of the austenite and HF-martensite surfaces with respect to the martensite one.

The final activation tests performed (Fig. 16) have confirmed the activation time repeatability in all configurations and again the good stress transfer capability of austenite.

4. Conclusions

The results coming from non-standard pull-out test show the efficiency of the embedding technique. The porting of the technology, originally developed for the embedding of OF, has proven its efficiency also for SMA-based composites. In addition, the direct constraint embedding technique of detwinned martensite wires allows the adoption of advanced composites as host materials. The results in terms of IFSS are encouraging considering that real peak values are much higher than recorded ones (which assumes a uniform stress distribution over the whole embedding length).

Standard pull-out tests have shown that higher load transfer capability is obtained when the wires are in the austenite phase (three times higher than martensite).

These considerations should be kept in mind in any future improvements of this embedding technique. Some preliminary studies showed that QP technique may overcome technological embedding difficulties. With this technique SMA wires can be embedded without constraints because of the detwinning being prevented by the cured QP. This improvement should be a very useful future development in terms of manufacturing and well-characterized actuators. This development must be subjected to a detailed interface analysis devoted to the optimization of materials and to the forming tools upgrade.

The limited invasivity of the developed QP with the composite host material is suggesting the implementation of this technology also in complex shape laminates.

References

1. I. Chopra, Review of State of Art Smart Structures and Integrated Systems, *AIAA J.*, 2002, **40**(11), p 2145–2187
2. S.P. Thompson and J. Loughlan, Adaptive Post Buckling Response of Carbon Fibre Plates Employing SMA Actuators, *Compos. Struct.*, 1997, **38**(1–4), p 667–678
3. Y.J. Zheng, L.S. Cui, and J. Schrooten, Basic Design Guidelines for SMA/Epoxy Smart Composites, *Mater. Sci. Eng. A*, 2005, **390**, p 139–143
4. P. Gaudenzi, M. Olivier, G. Sala, D. Sciacovelli, M. Wheelan, P. Bettini, G. Nosenzo, and A. Tralli, Development of an Active Composite with Embedded Piezoelectric Sensors and Actuators for Structure Actuation and Control, *Proceedings of the 54th International Astronautical*, IAC-03-I.4.03, Bremen, 2003
5. Q.P. Sun and K.C. Hwang, Micromechanics Modeling for the Constitutive Behavior of Polycrystalline Shape Memory Alloys, *J. Mech. Phys. Solids*, 1993, **I**, p 1–17, **II**, p 19–33
6. M. Cho and S. Kim, Structural Morphing Using Two-Way Shape Memory Effect of SMA, *Int. J. Solids Struct.*, 2005, **42**, p 1759–1776
7. M. Langelaar and F. van Keulen, Design Optimization of Shape Memory Alloy Structures, *10th AIAA/ISSMO Multidisciplinary Analysis and Optimization Conference* (Albany, NY), 2004
8. W. Huang, On the Selection of Shape Memory Alloys for Actuators, *Mater. Des.*, 2002, **23**, p 11–19
9. P. Bettini and G. Sala, Preliminary Assessment of Helicopter Rotor Blades Fatigue Endurance Through Embedded F.O. Sensors, *Proceeding of the 24th ICAF Symposium*, May 16–18 (Naples), 2007
10. D.A. Miller and D.C. Lagoudas, Thermo-Mechanical Characterization of NiTiCu and NiTi SMA Actuators: Influence of Plastic Strains, *Smart Mater. Struct.*, 2000, **9**(5), p 640–652
11. J. Khalil-Allafi, G. Eggeler, W. Schmahl, and D. Sheptyakov, Quantitative Phase Analysis in Microstructures which Display Multiple Step Martensitic Transformation in Ni-Rich NiTi Shape Memory Alloys, *Mater. Sci. Eng. A*, 2006, **438–440**, p 593–596
12. Z.G. Wang, X.T. Zu, X.D. Feng, S. Zhu, J.M. Zhou, and L.M. Wang, Annealing-Induced of Transformation Characteristics in TiNi Shape Memory Alloys, *Physica B*, 2004, **353**, p 9–14
13. ASTM F2004-03, Standard Test Method for Transformation Temperatures of Nickel-Titanium Alloys by Thermal Analysis
14. ASTM D3418-03, Standard Test Method for Transition Temperatures of Polymers by Differential Scanning Calorimetry
15. V. Birman, Stability of Functionally Graded Hybrid Composite Plates, *Compos. Eng.*, 1995, **5**(7), p 913–921
16. S.F. Zhandarov and E.V. Pisanova, The Local Bond Strength and Its Determination by Fragmentation and Pull-Out Tests, *Compos. Sci. Technol.*, 1997, **57**, p 957–964
17. C.Y. Yue, H.C. Looi, and M.Y. Quek, Assessment on Fibre-Matrix Adhesion and Interfacial Properties Using the Pull-Out Test, *Int. J. Adhes. Adhes.*, 1995, **15**(2), p 73–80
18. M.R. Piggot, Why Interface Testing by Single-Fibre Methods can be Misleading, *Compos. Sci. Technol.*, 1997, **57**, p 965–974
19. W. Beckert and B. Lauke, Critical Discussion of the Single Fibre Pull-Out Test: Does it Measure Adhesion?, *Compos. Sci. Technol.*, 1997, **57**, p 1689–1706